JPE 17-2-23

https://doi.org/10.6113/JPE.2017.17.2.551
ISSN(Print): 1598-2092 / ISSN(Online): 2093-4718

Effects of an Angle Droop Controller on the Performance of Distributed Generation Units with Load Uncertainty and Nonlinearity

M. S. Koupaei Niya†, Abbas Kargar*, and S. Y. Derakhshandeh*

†,*Department of Electrical Engineering, Shahrekord University, Chaharmahal and Bakhtiari Province, Iran

Abstract

The present study proposes an angle droop controller for converter interfaced (dispatchable) distributed generation (DG) resources in the islanded mode of operation. Due to the necessity of proper real and reactive power sharing between different types of resources in microgrids and the ability of systems to respond properly to abnormal conditions (sudden load changes, load uncertainty, load current disturbances, transient conditions, etc.), it is necessary to produce appropriate references for all of the mentioned above conditions. The proposed control strategy utilizes a current controller in addition to an angle droop controller in the discrete time domain to generate appropriate responses under transient conditions. Furthermore, to reduce the harmonics caused by switching at converters' output, a LCL filter is used. In addition, a comparison is done on the effects that LCL filters and L filters have on the performance of DG units. The performance of the proposed control strategy is demonstrated for multi islanded grids with various types of loads and conditions through simulation studies in the DigSilent Power Factory software environment.

Key words: Angle droop, Current controller, Current load disturbance, Discrete time, LCL filer, Load uncertainty

I. INTRODUCTION

The increased growth of DG can cause several problems for power networks. Problems which have arisen in the presence of distributed generators include:

1. Lack of proper control units results in stability problems under transient conditions.
2. Protection of DG units is very important in the grid connected mode.
3. The amount of power produced by DG units must guarantee an appropriate level of voltage, frequency control, amount of harmonic distortion, and reactive power supply.
4. The presence of DGs in distribution networks results in a loss of the network radial structure and a lack of coordination in the protective equipment.
5. The special features of DG units and their low inertia can result in technical and operational challenges in terms of the stability of power systems.
6. The incorrect positioning of these products can increase the losses in networks.
7. Distribution networks are designed with the assumption that the input of distribution substations is connected to a transmission grid which is the only source of power and short circuit capacity of networks. DG units, which put the power supply in different parts of the distribution network, are in violation of this assumption. As a result, these resources create situations that cannot occur in traditional networks.

Numerous studies have been done in this field to overcome these problems. Most modern DGs use a converter as an interface between the network and the sources. Therefore, most studies are focused on how to control these converters. Reference [1] proposed droop angle method to control the power output of a converter. It is assumed that there are two types of DG systems. Each system has its own local load, and it assumed that a microgrid is in the grid connected mode. In addition, [2] offered a method for improving the power division between DG units using an angle droop controller. In

Manuscript received Jan. 23, 2016; accepted Dec. 13, 2016
Recommended for publication by Associate Editor Alian Chen.
†Corresponding Author: saeed.koupaei@stu.sku.ac.ir
Tel: +98-7138436058, shahrekord university
*Department of Electrical Engineering, Shahrekord University, Iran

[3], [4], a comparison is made between angle droop and frequency droop. It is illustrated that angle droop shows a better overall performance. However, the effect of the proposed controller is not studied under unbalanced or nonlinear load conditions.

The coefficient of voltage droop can be defined as a function of the VSC active and reactive power outputs for the parallel operation of inverter-based DG systems [5]. In addition, converter systems can be equipped with active and reactive power controllers to optimize the behavior of the system under transient conditions. It must have the ability to maintain the angle stability and voltage quality of a microgrid within regions [6]. In practice, the proposed methods may not guarantee the control stability, robustness, or performance promised by the assumed models. Reference [7] investigated inverter-based DG systems in which the circuit and controller features can decrease or even increase the oscillations of a system.

To decrease the effects of load dynamics on the stability and performance of a system, based on a feed forward method, its DG units can be controlled. The design of the controller is easy in this method [8-10]. In addition, adaptive feedforward compensator can decrease the effects of load dynamics on DG units [11]. A control strategy has been proposed based on a mathematical discrete time model for the operation of a single dispatchable distributed generation unit [12]. This model is also applied to the performance of variable frequency DG units. However, adaptive control systems are highly nonlinear and time-varying. In addition, their stability requires the satisfaction of conservative constraints.

To remove the harmonics produced by converters, LCL filters are often used because of their better performance when compared to other types of filters. Moreover, these types of filters can be affordable. The main advantage of LCL filters over simple L filters is their effectiveness since L filters may attenuate only about 20db per decade over the whole frequency range [13]. LC filters such as network inductance have a variable resonant frequency in their lifetime. Therefore, these kinds of filters are not suitable for use in poor networks [14]. For LCL filter design, a method can be used so that the resonant frequency of the filter is set above the Nyquist frequency [15]. The switching frequency of converters is limited to 1 kHz because of the thermal limitations of semiconductors. This could limit the frequency band between the main and carrier frequency so that it is less than one-tenth of its real value. Therefore, the design of LCL-filters can be more challenging. In this case, a selective harmonic elimination bandwidth modulation method can be used, which eliminates low order harmonics and optimizes the LCL filter design [16]. Reference [17] proposed a harmonic model for LCL filters and then investigated the relationship between the parameters of the LCL filters, the resonance frequency, and ripple reduction at high frequencies. A method was proposed for the design of LCL filter parameters through an analysis of the current total harmonic distortion at the converter side inductance and a current ripple factor reduction injected into the network by the LCL filters [18]. Choosing appropriate parameters for LCL filters is also an affordable way to reduce switching harmonics at the grid side. Therefore, a cost function can be a criterion for LCL filter design [19]. A LCL filter traps topology can be used to design and analyze the filters used in high-power two-level converters, and this method can also be used for conventional LCL filters [20]. However, these methods bring extra control difficulties such as causing instability of the closed-loop control system.

The current study focuses on problems in the traditional control strategies. It uses a feedforward compensation method to change the dynamic interaction between DG units and a network. The proposed strategy behaves like a traditional droop controller. Therefore, it does not have any effect on the power division or voltage/frequency regulation. By changing the contribution of the load dynamics, the network stability increases. One problems is the impact of load current on the operation of a control system. This study uses a feedforward compensation for the removal of internal couplings and a reduction in the impact of load dynamics on the control system. Under these conditions, a closed loop system shows similar dynamic behavior under the no-load and loaded conditions. The present study uses the advantages of a PLL unit, which eliminates the need for external frequency measurements. It can also set up a control strategy under unusual circumstances and show robust properties under different switching conditions. The effects of balanced, unbalanced, and nonlinear load conditions are addressed. Sudden and random load switching incidents and short circuit events on the terminal voltage of a DG unit in the islanded mode operation of a microgrid system are also considered. Details of the mathematical modeling and controller design method in the discrete time domain are described. Moreover, to overcome the harmonics caused by converter switching, two types of filter are used. In addition, their effects on the performance of DG units are investigated. The impact of the proposed control strategy on network stability has been evaluated in the Digsilent Power Factory environment.

The rest of this paper is organized as follows. Section II describes the structure of an islanded network. Section III presents a mathematical model for DG units in the islanded mode of operation. Section IV illustrates a stability analysis of the controller. Section V presents simulation results to illustrate the effectiveness of the proposed strategy. Section VI concludes the paper.

II. Islanded Network and Distributed Generation Structure

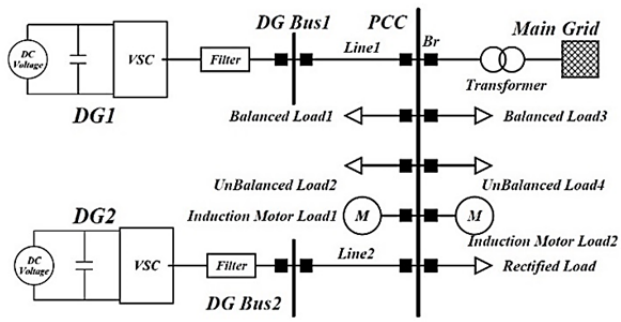

Fig. 1. Single line diagram of the test microgrid.

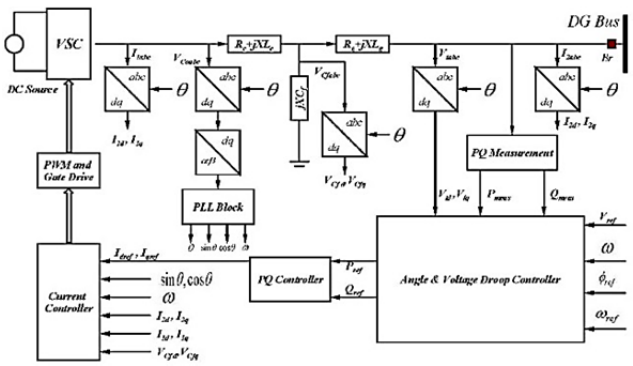

Fig. 2. Current control systems of the DG units with LCL filter.

Fig. 1 shows the general configuration of a microgrid. This microgrid can be applied in both the connected or islanded mode. DG units and loads are disconnected from the main grid if the Br switch is tripped. In the connected mode, the outputs of the DG units are delivered by transformers to the main grid, and a part of the local loads can be provided by these units. The network of Fig. 1 consists of two converter interfaced (dispatchable) DGs, and the outputs for each of the DG units are connected to the main bus (PCC) through transmission lines which supply four types of local loads. These loads are: 1) balanced three-phase loads; 2) induction motor loads; 3) unbalanced loads; and 4) rectified loads. Each of these loads can be connected through a transformer to the main bus.

Fig. 2 illustrates the control unit of a single DG unit. The DG unit has a voltage source converter supplied by a DC source. The DC supply represents an energy storage or the rectified DG output of a dispatchable generator. Switching signals are provided for the voltage source converter through a current controller. In this controller, a three-phase system to a d-q two axis system transformation is used where θ is the d axis degree with respect to the stationary axis α.

This angle is provided by a PLL block. Another output of this block is the frequency generated by the DG units. The three phase variables I_{1abc}, I_{2abc}, V_{Cabc}, V_{Cfabc}, and V_{tabc} represent the converter, the network side current of the LCL filter, the converter side, the capacitor voltage of the LCL filter, and the PCC bus voltage, respectively. The purpose of this filter is to smooth the output voltage and to remove the

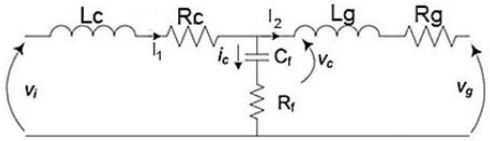

Fig. 3. Single phase model of the LCL filter.

harmonics produced by the converter. The parameters of this filter can be obtained by the method introduced in references [21], [22]. Fig. 3 shows a filter per-phase model, where R_C, L_C, R_g, and L_g represent the resistor and inductor of the converter, and of the grid-side of the LCL filter, respectively. R_f and C_f represent the damping resistor and capacitor of this filter.

To produce references for the active and reactive powers, the bus power of the DG units, the voltage, and the frequency of the filter grid side are measured and sent to the angle and voltage droop controller block. In the Angle Droop Controller, the voltage angle is compared with its reference value. Angle (1) can be used to generate a reference [6].

$$\varphi^* = (\omega_S - (m \times P) - \omega_{PCC}) K_I / S + \omega_{PCC} / S \quad (1)$$

Where Φ*, ωs, ω, PCC, m, P, and KI are the reference angles, measured frequency, reference frequency, droop coefficient, measured active power, and integral factor, respectively. Fig. 4 shows a method for obtaining a reference angle.

Differences between the measured and reference values of the voltage and angle are used to produce the active and reactive power references based on (2) in the angle and voltage droop controller block.

$$\begin{aligned} \delta &= \delta_{Rated} - m(P_{Rated} - P) \\ V &= V_{Rated} - n(Q_{Rated} - Q) \end{aligned} \quad (2)$$

Where δ_{rated}, δ, P_{rated}, P, Q_{rated}, Q, V_{rated}, V, and m, n represent the reference angle, the produced angle, the reference and measured active and reactive power, the reference and measured voltage, and the droop coefficient, respectively. The outputs of the block are then sent to the PQ controller unit to produce a reference current for converter switching through the PLL block outputs.

In the connected mode of operation, the voltage and frequency of the microgrid are influenced by the main gird. The islanded mode occurs when the Br switch is tripped. In this mode of operation, the DG units are responsible for the provision of loads and for maintaining the voltage and frequency of the grid. Therefore, a control method is needed to regulate the actual amplitude and frequency of the bus voltages under various conditions.

III. Current Control Strategy

In order to eliminate the harmonics produced by a converter, this study considers LCL and L filters at the outputs of the DG units. The effects of these filters on the

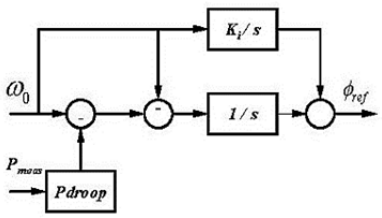

Fig. 4. Production of the reference angle.

performance of the DG units are investigated through discrete time equation in parts A and B.

A. Current Angle Droop Control Strategy with an LCL Filter

The current control strategy includes the core shown in Fig. 2. The main purpose of the current controller is the adjustment of the current components at the ac-side of VSC by means of pulse width modulation. To analyze how the required pulses are produced in different situations, the continuous-time state equations of the grid and converter side currents of LCL filter in Fig. 2 are defined as follows:

$$\begin{aligned} L_c \frac{dI_1}{dt} + R_c I_1 + V_{Cf} &= U \\ L_g \frac{dI_2}{dt} + R_g I_2 + V_t &= V_{Cf} \end{aligned} \tag{3}$$

In (3), I_1, I_2, V_{Cf}, and V_t represent the three-phase state vectors of the LCL filter network and converter side currents, the capacitor voltage of the filter, and the DG unit output voltage, respectively. The converter side voltage of the LCL filter is controlled by PWM signals of the VSC based on U signal. The state equations expressed in (3) can be transformed into two axis d-q rotating forms according to $\overrightarrow{R(t)} = \left(R_d(t) + jR_q(t)\right)e^{j\theta}$. Therefor a d-q rotating form of (3) can be obtained as follows.

$$\begin{aligned} &L_c \frac{d}{dt}\left(I_{1d} + jI_{1q}\right)e^{j\theta} + R_c\left(I_{1d} + jI_{1q}\right)e^{j\theta} \\ &\quad + \left(V_{Cfd} + jV_{Cfq}\right)e^{j\theta} = \left(U_d + jU_q\right)e^{j\theta} \\ &L_g \frac{d}{dt}\left(I_{2d} + jI_{2q}\right)e^{j\theta} + R_g\left(I_{2d} + jI_{2q}\right)e^{j\theta} \\ &\quad + \left(V_{td} + jV_{tq}\right)e^{j\theta} = \left(V_{Cfd} + jV_{Cfq}\right)e^{j\theta} \end{aligned} \tag{4}$$

A simplified model of (4) can be expressed as follows.

$$\begin{aligned} L_c \frac{d}{dt} I_{1d} &= -R_c I_{1d} + V_{Cfd} + L_c \omega I_{1q} + U_d \\ L_c \frac{d}{dt} I_{1q} &= -R_c I_{1q} + V_{Cfq} - L_c \omega I_{1d} + U_q \end{aligned} \tag{5}$$

$$\begin{aligned} L_g \frac{d}{dt} I_{2d} &= -R_g I_{2d} - V_{td} + L_g \omega I_{2q} + V_{Cfd} \\ L_g \frac{d}{dt} I_{2q} &= -R_g I_{2q} - V_{tq} - L_g \omega I_{2d} + V_{Cfq} \end{aligned} \tag{6}$$

In (5) and (6), ω is the PLL block output and its relationship with the angle θ is as follows.

$$\frac{d\theta}{dt} = \omega \tag{7}$$

V_{Cfd} and V_{Cfq} can be obtained from (5) and (6) as follows.

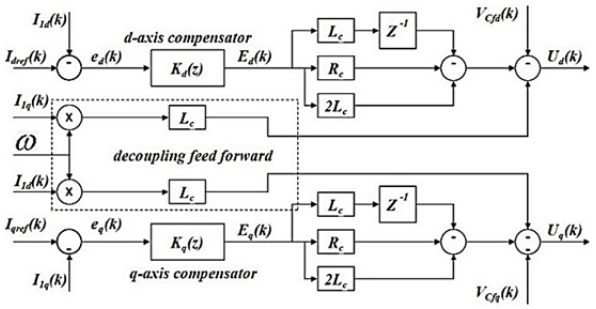

Fig. 5. Current control of DG unit with LCL filter.

$$\begin{aligned} V_{Cfd} &= L_g \frac{d}{dt} I_{2d} + R_g I_{2d} + V_{td} - L_g \omega I_{2q} \\ V_{Cfq} &= L_g \frac{d}{dt} I_{2q} + R_g I_{2q} + V_{tq} + L_g \omega I_{2d} \end{aligned} \tag{8}$$

By substituting (8) into (5) it is possible to deduce the following.

$$\begin{aligned} L_c \frac{d}{dt} I_{1d} &= -R_c I_{1d} + \underbrace{L_g \frac{d}{dt} I_{2d} + R_g I_{2d} + V_{td} - L_g \omega I_{2q} + L_c \omega I_{1q} + U_d}_{\lambda_d} \\ L_c \frac{d}{dt} I_{1q} &= -R_c I_{1q} + \underbrace{L_g \frac{d}{dt} I_{2q} + R_g I_{2q} + V_{tq} + L_g \omega I_{2d} - L_c \omega I_{1d} + U_q}_{\lambda_q} \end{aligned} \tag{9}$$

Using $A_d(T)=e^{AT}$,$B_d(T)=(\int e^{AT}\, d\tau)B$ to convert (9) from continuous to discrete-time, it is possible to obtain the following.

$$\begin{aligned} I_{1d}(k+1) &= aI_{1d}(k) + b\lambda_d(k) \\ I_{1q}(k+1) &= aI_{1q}(k) + b\lambda_q(k) \end{aligned} \tag{10}$$

The *a* and *b* parameters can be obtained by.

$$\begin{aligned} I_{1d}(k+1) &= aI_{1d}(k) + b\lambda_d(k) \qquad a = e^{-\frac{R_c T_s}{L_c}} \\ I_{1q}(k+1) &= aI_{1q}(k) + b\lambda_q(k) \qquad b = -\frac{1}{R_C}\left(e^{-\frac{R_c T_s}{L_c}} - 1\right) \end{aligned} \tag{11}$$

In (11), T_S represents a sampling period. In order to obtain $I_{1d}(k)$,$I_{1q}(k)$, at each step of k in (9), it is necessary to specify $I_{2d}(k+1)$,$I_{2q}(k+1)$. To estimate the (k+1)th value of these variables, $x(k+1)\approx 2x(k)-x(k-1)$ can be used [23]. Equations (3) to (11) represent the current control scheme with a LCL filter whose block diagrams are shown in Fig. 5 and Fig. 6. In Fig. 5, $I_{1d}(k)$,$I_{1q}(k)$, $I_{2d}(k)$,$I_{2q}(k)$, and $U_d(k)$,$U_q(k)$ are output and input signals of this control plant.

Fig. 5 illustrates that in order to regulate the output voltage and frequency of the DG units, the error signals $e_d(k)=I_{dref}(k)-I_{1d}(k)$ and $e_q(k)=I_{qref}(k)-I_{1q}(k)$ should be processed to produce the $U_d(k)$ and $U_q(k)$ signals necessary for the control scheme. To process the error signals, $K_d(z)$ and $K_q(z)$ blocks are used. In these two blocks, a simple PI compensator can be used to eliminate the steady state error signal.

B. Current Angle Droop Control Strategy with a L Filter

In this part, the impact of a L type filter on the DG unit output is studied. In order to recognize the effect filter type has on the DG unit outputs, a comparison is done between the

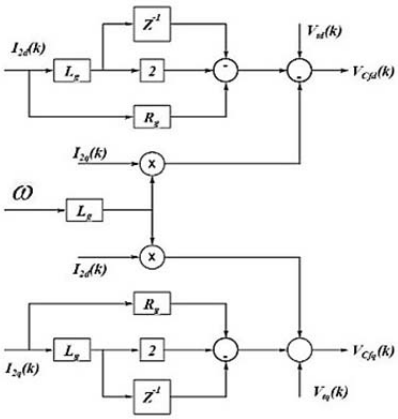

Fig. 6. Capacitor voltage of DG unit with LCL filter.

outputs of these two filters. Fig. 7 illustrates a control system for distributed generation with a L filter. In accordance with the described contents, continuous time state equations of a system with a L filter are expressed. They are similar to (3)-(6).

$$L_c \frac{d}{dt} I_{1d}(k) = -R_c I_{1d}(k) + V_{td}(k) + \frac{L_c \omega(k) I_{1q}(k) + U_d(k)}{\lambda_d}$$
$$L_c \frac{d}{dt} I_{1q}(k) = -R_c I_{1q}(k) + V_{tq}(k) + \frac{L_c \omega(k) I_{1d}(k) + U_q(k)}{\lambda_q} \quad (12)$$

By transforming (12) into discrete time it is possible to deduced that:

$$I_{1d}(k+1) = aI_{1d}(k) + b\beta_d$$
$$I_{1q}(k+1) = aI_{1q}(k) + b\beta_q \quad (13)$$

The values of a and b can be obtained by (11). In addition, the parameters β_d and β_q can be defined as:

$$\beta_d = \frac{T_s}{C_f}\lambda_d(k) + \lambda_d(k) + V_{td}(k)$$
$$\beta_q = \frac{T_s}{C_f}\lambda_q(k) + \lambda_q(k) + V_{tq}(k) \quad (14)$$

A DG unit current control block with a L filter is shown in Fig. 5 except that V_{cf} is replaced with the terminal voltage V_t. The rest of the blocks are the same as those of the LCL filter.

IV. Stability Analysis of a Controller with a LCL Filter

According to the network, the impedance value as seen from the LCL filter can be expressed as follows [24].

$$G_{net} = \frac{s^3 L_c L_g C + s^2 (L_c R_g + R_c L_g + KL_g)C}{s^2 L_c C + s(KC + R_c C) + 1} + \frac{s(RcRgC + KRgC + Lc + Lg) + Rc + Rg}{s^2 L_c C + s(KC + R_c C) + 1} \quad (15)$$

Where, L_c, R_c, L_g, R_g, and C represent the resistor and inductor of converter and grid-side of LCL filter, and capacitor of LCL filter, respectively. The effects of the controller on the impedance value can be expressed by:

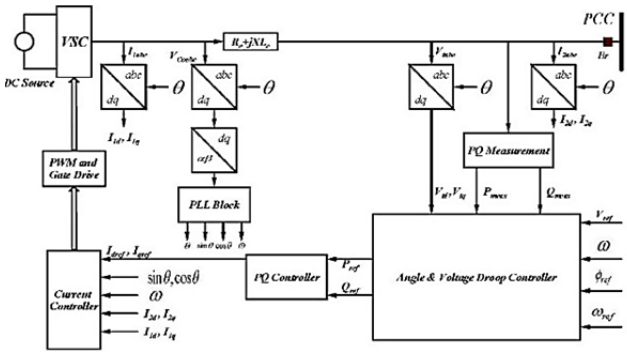

Fig. 7. Current control systems of the DG units with L filter.

$$G_{Total} = G_{net} + G_{PI} \quad (16)$$

Where G_{PI} is the controller transfer function. A high grid impedance at a given frequency, can ensure a small percentage of voltage disturbances at the grid current.

$$G_{Total} = \frac{s^3 L_c L_g C + s^2 (L_c R_g + R_c L_g + KL_g)C}{s^2 L_c C + s(KC + R_c C) + 1} + \frac{s(RcRgC + KRgC + Lc + Lg) + Rc + Rg}{s^2 L_c C + s(KC + R_c C) + 1} + \frac{1}{s^2 L_c C + s(KC + R_c C) + 1}(K_p + \frac{K_I}{s}) \quad (17)$$

Due to the penetration of the digital controller into the power system, the continuous time signal should be converted into discrete time. To keep the samples fixed in each period, which is required for the optimal performance of the controller, the sampling period is locked to the signals' period to produce a fixed number of samples per cycle, which means that $N = {}^{T}/_{T_s}$ is always constant. Where, T_s and T represent the sampling and signal periods, respectively. In the present study, N is chosen to be 4. The main parameter, which has the greatest effect on the stability of G_{Total}, is K, and it is chosen to be 9 in this study. The discrete time model of (17) can be obtained as follows [25].

$$H(z) = \frac{9.02T\left(Z + e^{-1.23\times10^4 T}\right)}{Z - e^{-1.23\times10^4 T}} + \frac{3.6T\left(Z + e^{-1.22\times10^4 T}\right)}{Z - e^{-1.22\times10^4 T}} + \frac{1.6TZ^2 - 11.3Te^{-1.2\times10^4 T}\cos(-1.43 - 61T)Z}{Z^2 - 2e^{-1.2\times10^4 T}\cos(61T)Z + e^{-2\times1.2\times10^4 T}} + \frac{0.04T\left(Z + e^{-1265T}\right)}{Z - e^{-1265T}} + \frac{8.5TZ^2 - 10.04Te^{-1.21\times10^4 T}\cos(0.5608 - 34T)Z}{Z^2 - 2e^{-1.21\times10^4 T}\cos(34T)Z + e^{-2\times1.21\times10^4 T}} + 0.006T + \frac{1206TZ^2 - 1270Te^{-5T}\cos(-0.32 - 3760T)Z}{Z^2 - 2e^{-5T}\cos(3760T)Z + e^{-2\times5T}} + \frac{0.0244TZ^2 - 0.0302Te^{-1270T}\cos(-0.63 - 20T)Z}{Z^2 - 2e^{-1270T}\cos(20T)Z + e^{-2\times1270T}} + \frac{0.0132TZ^2 - 0.042Te^{-1267T}\cos(1.25 - 30T)Z}{Z^2 - 2e^{-12267T}\cos(30T)Z + e^{-2\times12267T}} + \frac{2.1TZ^2 - 2.41Te^{-16T}\cos(0.52 - 8T)Z}{Z^2 - 2e^{-16T}\cos(8T)Z + e^{-2\times16T}} - 1 \quad (18)$$

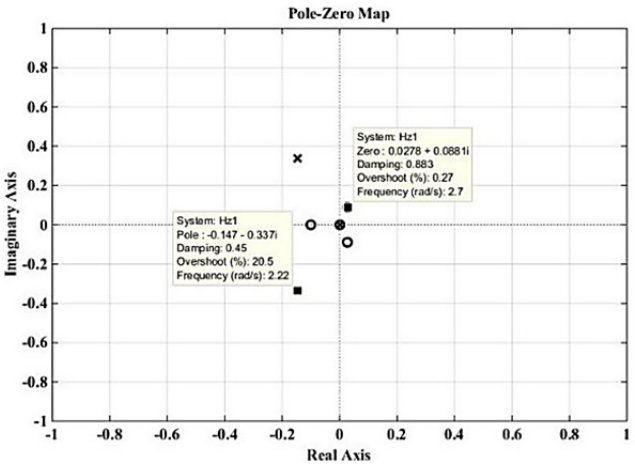

Fig. 8. Closed loop system pole zero plot (K=9).

Where, T represent sampling period. Fig. 8 illustrates the location of the poles and zeroes of the whole discrete-time closed-loop transfer function of the system for N= 4 and K=9.

V. CASE STUDY AND SIMULATION RESULTS

To show the effectiveness of the control strategies described in the previous sections, Fig. 1 shows the switching details simulated in the Digsilent Power Factory environment. The parameters of the lines and DG units used in a microgrid are presented in the Appendix. In order to design the LCL parameters, the procedures expressed in [21, 22] can be applied. The design parameters of the LCL filter are provided in the Appendix. The performance of this control system is also investigated with a L filter. Hence the filter parameters are designed based on the procedure expressed in [26]. The loads connected to the microgrid of Fig. 1 consist of a balanced three-phase load, an unbalanced load, and rectified and induction motor loads. The values for each of the loads are given in the Appendix.

In this case study, the balanced loads are connected to the microgrid from the start up time of the simulation. In addition, all of the loads of the microgrid in the connected mode are provided by the main grid. At t=10s, the Br switch is opened, and from this point, the DG units are responsible, based on their droop coefficients, for the provision of loads. The series of events investigated in this microgrid are given in Table I. These events have been chosen to illustrate the behavior of the proposed control strategy.

A. System Response in the Presence of a Conventional Angle Droop Controller

As stated previously, the effects of uncertainties and nonlinearities in the loads and fault conditions such as short circuit events, are not investigated in the conventional angle droop controller. The performance of this controller is evaluated under a short circuit event. A three-phase short circuit is created at t = 28s at line 1 of Fig. 1. To remove this fault, the line is disconnected after 0.16 sec. Fig. 9 shows the voltage and frequency of the PCC bus in the presence of a conventional angle controller. As this figure shows, at time t=32s, after reconnecting line 1, the network leads to instability. In order to solve this problem, the proposed controller can be used.

TABLE I
SERIES OF EVENTS INVESTIGATED IN MICROGRID

Item	Event type	Time (sec)
1	Disconnecting from main grid	10
2	Operation of controller strategy	10
3	Connecting rectified load	15
4	Connecting M1,M2	20
5	Connecting Load2 & Load4	25
6	short circuit event in line 1	28
7	Disconnecting Line 1	28.16
8	reconnecting Line 1 to microgrid	32
9	Opening phase a of Line1	35
10	Close phase a of Line1	41
11	Disconnecting Load2 & Load4	45
12	Changing reference voltage from 1 to 0.95 p.u	55

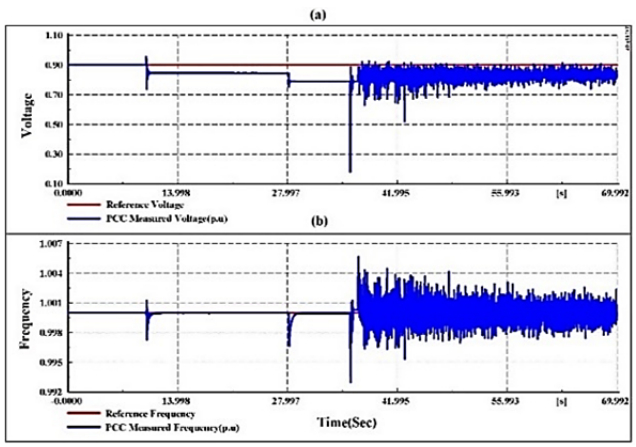

Fig. 9. a- PCC bus voltage b-PCC bus frequency in the presence of conventional controller.

B. System Response to the Mode Transfer of a Microgrid

In this section, the proposed control behavior and the impact of the filter type on the DG unit outputs are investigated. The following figures illustrate the impact of these two types of filters on the output of the DG unit at the same time.

After the Br switch in Fig. 1 is opened, the DG units supply three-phase balanced loads. Fig. 10 and Fig. 11 illustrate that during the islanding mode, the voltage and frequency for both of the DG units track their references at steady and appropriate speeds. This condition also exists when the motor and unbalanced loads are connected to the grid at 20 and 25 second, respectively.

As the figures shows, the proposed control strategy can force the DG units to track their references at stable and appropriate speeds in less than 0.5 sec.

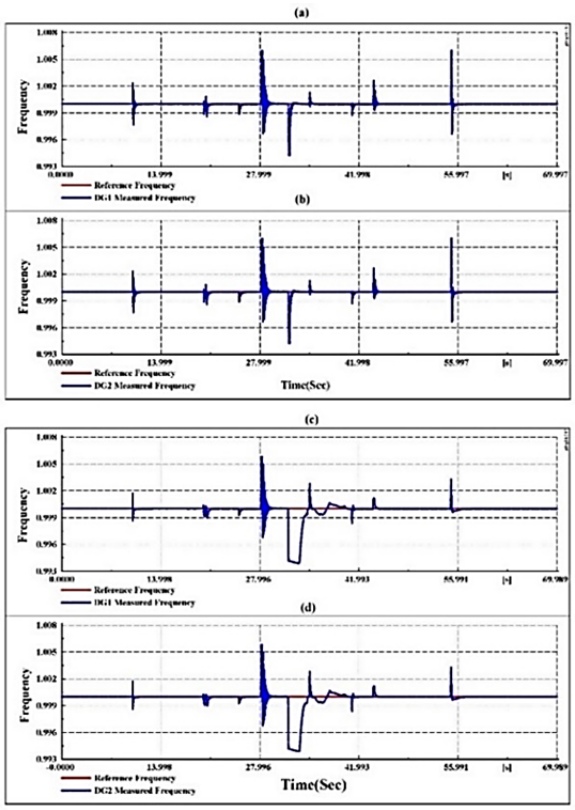

Fig. 10. Reference and measured frequency - a DG #1 with LCL filter b- DG #2 with LCL filter c-DG #1 with L filter d- DG #2 with L filter.

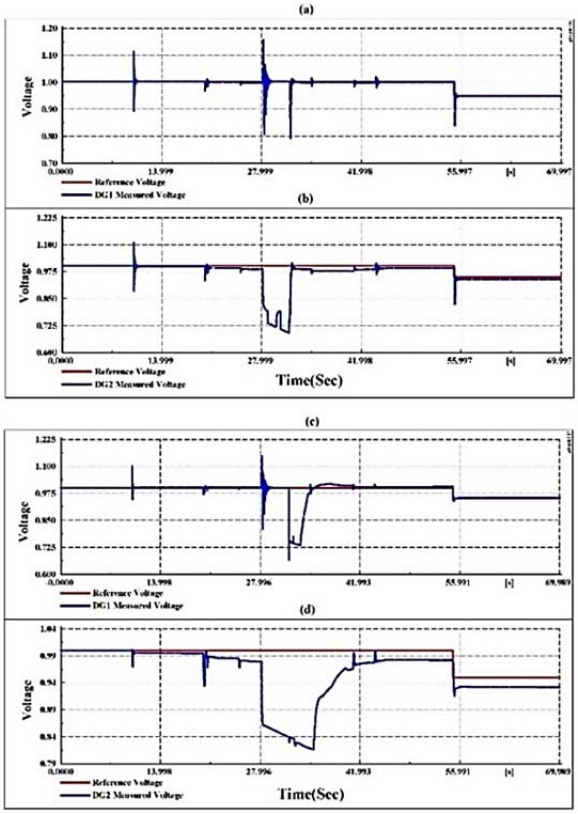

Fig. 11. Reference and measured voltage - a DG #1 with LCL filter b- DG #2 with LCL filter c-DG #1 with L filter d- DG #2 with L filter.

C. Response to a Load Current Disturbance

One type of load considered in Fig. 2 is a rectified load which is a three-phase full-wave rectifier circuit using thyristors as the switching element. In this case study, the rectifier is switched on at t=15s. It should be noted that at this time, the balanced loads are still connected to the grid. In addition, the DG units should supply both balanced and rectified loads.

D. Response to a Short Circuit Event and a Change in the Circuit Topology

At t=27s, a three phase short circuit occurs at the transmission line connected to DG unit #1. To remove the fault, this line is disconnected after 0.16 sec, and from this time, DG unit #2 is responsible for the provision of loads. As shown in Fig. 10 and Fig. 11, the control system forces DG unit #2 to track its references at a stable and appropriate speed. To maintain the system frequency, DG unit #2 is forced to produce active power beyond its rated capacity. Therefore, the ability to produce reactive power needed to maintain the system voltage at the reference value is reduced. Accordingly, the voltage of the converter bus is dropped 0.175p.u. This problem is reflected on the PCC bus voltage and frequency (Fig. 12). In order to fix this problem, a load shedding should be done in accordance with the importance of the loads to compensate for the voltage drop. At this time, the voltage of DG unit #1 remains at its reference value. It should be noted that the transient condition settles down in less than 2.5 sec. After the fault is cleared, at t=32s, DG unit #1 is reconnected. It can be seen that the control system settled down the transient condition in less than 3 sec.

E. Response to a Single Phase Trip of a Line

At t=35s, a single phase trip occurs at the circuit breaker of line1. As shown in the figures, the proposed control strategy can force the DG units to track their references at a stable and appropriate speed.

F. Response to Changes in the Voltage Reference

At t=55s, the reference voltage is decreased about 0.05 p.u, and the system control forces the DG units to follow their frequency and voltage references with a stable and appropriate speed. It takes about 1.5 sec to settle down the transient condition. Fig. 13 shows active and reactive power sharing between the DG units under different conditions.

Fig. 13-a and c show that active power sharing is done based on the droop coefficient, and that power output of DG unit #1 is greater than that of DG unit #2. This power sharing is done in a stable manner and at an appropriate speed under all conditions. Considering the reactive power sharing due to the R/X ratio of the transmission line, this ratio is more than 1 in the distribution network, unlike the droop coefficient. DG

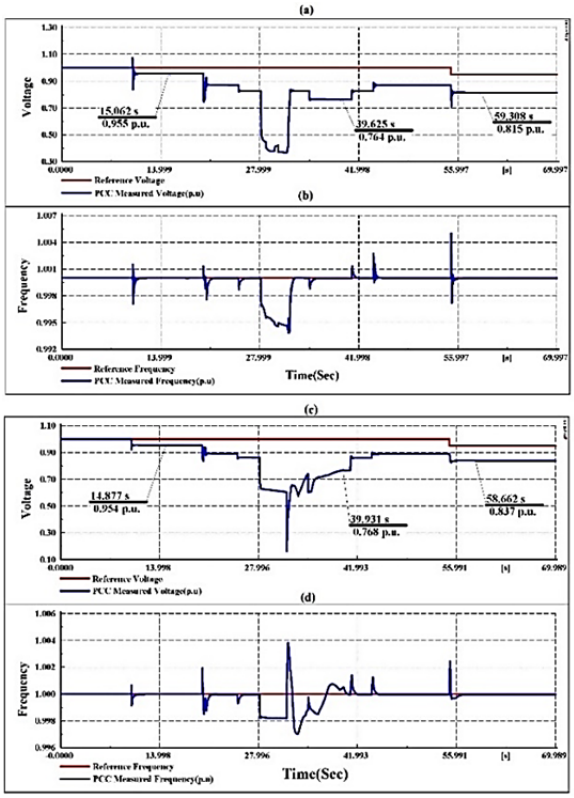

Fig. 12. a-PCC voltage with LCL filter b- PCC frequency with LCL filter c-PCC voltage with L filter d- PCC frequency with L filter.

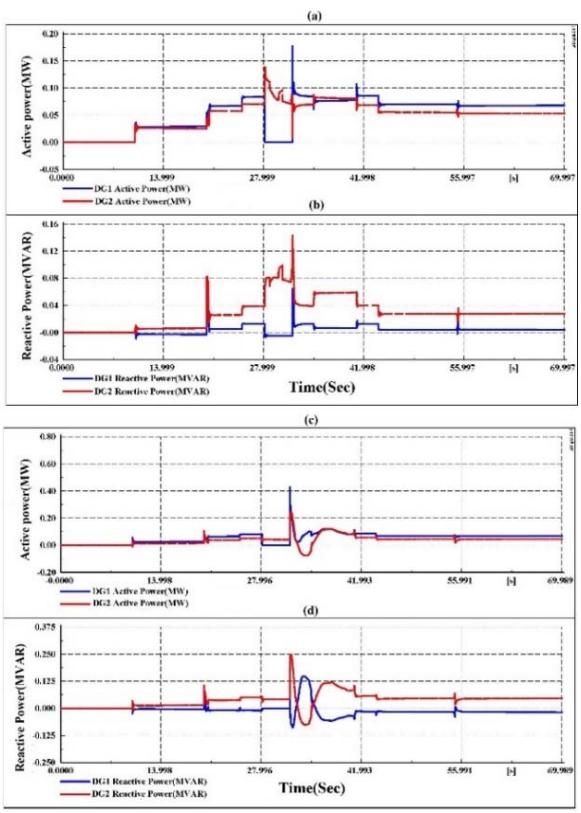

Fig. 13. a-active power sharing between DG units with LCL filter - b-reactive power sharing between DG units with LCL filter c-active power sharing between DG units with L filter - d-reactive power sharing between DG units with L filter.

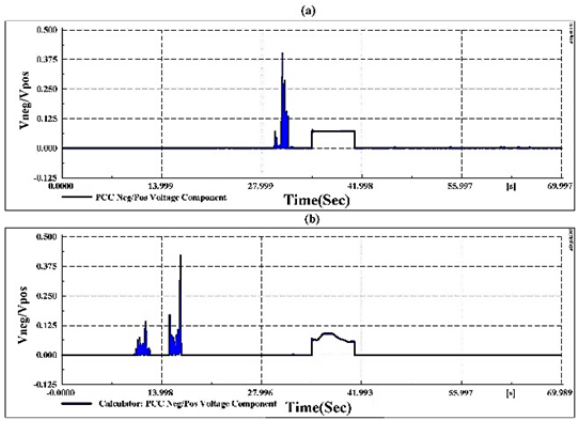

Fig. 14. Overall ratio of Neg/Pos Sequence of PCC Voltage- a with LCL filter b- with L filter.

unit #2 has a larger part than DG unit #1 in the provision of microgrid reactive power. By increasing the inductance of the lines when compared with the resistance property, the reverse mode is created in the reactive power sharing.

For the maximum ratio of $^{VPCC_{Neg}}/_{VPCC_{pos}}$, which occurs during the time of the DG unit#1 outage, this ratio is below 40% which refers to the low imbalance condition (Fig. 13). For other simulation times, this ratio is even lower than 20%. These numbers demonstrate the effectiveness of the proposed control strategy.

VI. Conclusion

The current study proposed an angle droop controller for the converters of dispatchable DG units connected to a network. Various types of loads including an induction motor load, an unbalance load, and load current disturbance are considered to demonstrate effectiveness of the proposed control strategy. This strategy ensures proper load sharing between all of the DG units via utilizing a current controller with an angle droop controller in all of the loads. A LCL type filter may eliminate the harmonics produced by the interface converters. The overall effectiveness of the proposed control strategy was studied in detail with several loads and transient conditions. In addition, a comparison was done between two types of filters. The results reveal the good effect a LCL filter has on the performance of an overall control system when compared with a L filter.

Appendix

TABLE II
Parameters of DG Units Used in Microgrid

DG Parameters		
Parameter	DG #1	DG #2
m (p.u)	0.0167	0.02
n (p.u)	0.0333	0.04
S (KVA)	120	100
Voltage (V)	400	400

TABLE III
PARAMETERS OF LINES USED IN MICROGRID

Line parameter	Line	Line1
R(Ω/Km)	0.1	0.1
XL(Ω/Km)	0.02	0.02
Length(km)	3	2
Voltage(V)	400	400

TABLE IV
ACTIVE AND REACTIVE LOAD VALUES OF PCC BUS

		P(KWatt)	Q(KVar)
Load1		22	4
Load3		30	5
M1,M2		3	4
Load2	Phase a	10	5
	Phase b	0	0
	Phase c	15	6
Load4	Phase a	0	0
	Phase b	10	6
	Phase c	17	4
Rectified Load		40	5

TABLE V
DESIGN PARAMETERS OF LCL & L FILTER

Parameter	Remark	Value	
$\mathbf{f_g}$	Grid frequency	50	
$\mathbf{f_{SW}}$	Switching frequency	10 KHz	
LCL Filter		DG #1	DG #2
$\mathbf{L_C}$ **(mh)**	Converter-side inductance	0.68	0.817
$\mathbf{L_g}$ **(μh)**	Grid-side inductance	15.91	19.12
$\mathbf{C_f}$	Filter capacitance	95.5	79.5
$\mathbf{R_f}$	Damping resistance	0.1345	0.162
$\mathbf{R_C}$	Converter-side resistance	0.12	0.15
$\mathbf{R_g}$	Grid-side resistance	0.015	0.017
L Filter			
L (mh)	Filter inductance	1.282	1.53

REFERENCES

[1] R. Majumder, A. Ghosh, G. Ledwich, and F. Zare, "Load sharing and power quality enhanced operation of a distributed microgrid," *IET Renew. Power Gener.,* Vol. 3, No. 2, pp. 109-119, Jun. 2009.

[2] R. Majumder, A. Ghosh, G. Ledwich, and F. Zare, "Improvement of stability and load sharing in an autonomous microgrid using supplementary droop control loop," *IEEE Trans. Power Systems,* Vol. 25, No. 2, pp. 796-808, May 2010.

[3] R. Majumder, A. Ghosh, G. Ledwich, and F. Zare, "Operation and control of hybrid microgrid with angle droop controller," *IEEE Region 10 Conference,* pp. 509-515, 2010.

[4] R. Majumder, A. Ghosh, G. Ledwich, and F. Zare, "Angle droop versus frequency droop in a voltage source converter based autonomous microgrid," *PES '09. IEEE Power & Energy Society General Meeting,* pp. 1-8, 2009.

[5] E. Rokrok and G. M. E. H., "Adaptive voltage droop scheme for voltage source converters in an islanded multibus microgrid," *IET Gener. Transm. Distrib,* Vol. 4, No. 5, pp. 562-578, May 2010.

[6] N. Pogaku, M. Prodanovic, and T. C. Green, "Modeling, analysis and testing of autonomous operation of an inverter-based microgrid," *IEEE Trans. Power Electron.,* Vol. 22, No. 2, pp. 613-625, Mar. 2007.

[7] M. B. Delghavi and A. Yazdani, "A control strategy for islanded operation of a distributed resource (DR) unit," *PES '09. IEEE Power & Energy Society General Meeting,* pp. 1-8, 2009.

[8] M. B. Delghavi and A. Yazdani, "An adaptive feed forward compensation for stability enhancement in droop-controlled inverter-based microgrids," *IEEE Trans. Power Del.,* Vol. 26, No. 3, pp. 1764-1773, Jul. 2011.

[9] M. B. Delghavi and A. Yazdani, "Islanded-mode control of electronically coupled distributed-resource units under unbalanced and nonlinear load conditions," *IEEE Trans. Power Del.,* Vol. 26, No. 2, pp. 661-673, Apr. 2011.

[10] M. B. Delghavi and A. Yazdani, "A unified control strategy for electronically interfaced distributed energy resources," *IEEE Trans. Power Del.,* Vol. 27, No. 2, pp. 803-812, Apr. 2012.

[11] R. Majumder, A. Ghosh, G. Ledwich, and F. Zare, "Control of parallel converters for load sharing with seamless transfer between grid connected and islanded modes," *IEEE Conference in Power and Energy Society General Meeting,* pp. 1-7, 2008.

[12] V. Blasko and V. Kaura, "A novel control to actively damp resonance in input LC filter of a three-phase voltage source converter," *IEEE Trans. Ind. Appl.,* Vol. 33, No. 2, pp. 542-550, Mar./Apr. 1997.

[13] M. Raoufi and M. T. Lamchich, "Average current mode control of a voltage source inverter connected to the grid: Application to different filter cells," *Journal of Electrical Engineering,* Vol. 55, pp. 77-82, 2004.

[14] J. San-Sebastian, I. Etxeberria-Otadui, A. Rujas, J. A. Barrena, and P. Rodriguez, "Optimized LCL filter design methodology applied to MV grid-connected multimegawatt VSC," *IEEE Energy Conversion Congress and Exposition (ECCE),* pp. 2506 - 2512, 2012.

[15] Y. Tang, W. Yao, P. C. Loh, and F. Blaabjerg, "Design of LCL-filters with LCL resonance frequencies beyond the nyquist frequency for grid-connected inverters," *IEEE Energy Conversion Congress and Exposition (ECCE), 2015*, 2015.

[16] M. Zabaleta, E. Burguete, D. Madariaga, I. Zubimendi, M. Zubiaga, and I. Larrazabal, "LCL grid filter design of a multi-megawatt medium-voltage converter for offshore wind turbine using SHEPWM modulation," *IEEE Trans. Power Electron.,* Vol. 31, No. 3, pp. 1993-2001, Mar. 2016.

[17] F. Liu, X. Zha, Y. Zhou, and S. Duan, "Design and research on parameter of lcl filter in three-phase grid-connected inverter," *IEEE 6th International Power Electronics and Motion Control Conference, 2009. IPEMC '09,* pp. 2174-2177, 2009.

[18] M.-Y. Park, M.-H. Chi, J.-H. Park, H.-G. Kim, T.-W. Chun, and E.-C. Nho, "LCL-filter design for grid-connected PCS using total harmonic distortion and ripple attenuation

factor," *IEEE International Power Electronics Conference (IPEC),* pp. 1688-1694, 2010.
[19] B.-G. Cho, S.-K. Sul, H. Yoo, and S.-M. Lee, "LCL filter design and control for grid-connected PWM converter," *IEEE 8th International Conference on Power Electronics and ECCE Asia (ICPE & ECCE),* pp. 756-763, 2011.
[20] A. M. Cantarellas, E. Rakhshani, D. Remon, and P. Rodriguez, "Design of passive trap-LCL filters for two-level grid connected converters," *IEEE 15th European Conference on Power Electronics and Applications (EPE),* pp. 1-9, 2013.
[21] A. Reznik, M. G. Simões, A. Al-durra, and S. M. Muyeen, "LCL filter design and performance analysis for small wind turbine system ms," in *Power Electronics and Machines in Wind Applications (PEMWA),* pp. 1-7, 2012.
[22] A. Reznik, M. G. Simões, A. Al-Durra, and S. M. Muyeen, "LCL filter design and performance analysis for grid interconnected systems," *IEEE Trans. Ind. Appl.,* Vol. 50, No. 2, pp. 1225-1232, Mar./Apr. 2014.
[23] T. Kawabata, T. Miyashita, and Y. Yamamoto, "Dead beat control of three phase PWM inverter," *IEEE Trans. Power Electron,* Vol. 5, No. 1, pp. 21-28, Jan. 1990.
[24] R. Chattopadhyay, A. De, and S. Bhattacharya, "Comparison of PR controller and damped pr controller for grid current control of LCL filter based grid-tied inverter under frequency variation and grid distortion," *IEEE Energy Conversion Congress and Exposition (ECCE),* pp. 3634-3641, 2014.
[25] M. Corinthios, *Signals, systems, transforms, and digital signal processing with MATLAB*: CRC Press, 2009.
[26] P. B.C, "Integrated approach to filter design for grid connected power converters," M.S. Thesis, Department of Electrical Engineering, Indian Institute of Science, India, 2009.

M. S. Koupaei Niya was born in March 1978, in Tehran, Iran. He received his B.S. degree in Electrical Engineering from Shiraz University, Shiraz, Iran, in May 2002; and his M.S. degree from Tehran University, Tehran, Iran, in 2005. He is presently working towards his a Ph.D. degree in the Department of Electrical Engineering, Shahrekord University, Chaharmahal and Bakhtiari Province, Iran. For 5 years he worked as a HV designer of substation post at the Fars Consulting Engineering Company, Shiraz, Iran. His current research interests include power system planning, operation and optimal control, microgrids, renewable energy resources and systems, and smart grids.

Abbas Kargar was born in Jahrom, Iran. He received his B.S., M.S. and Ph.D. degrees in Electrical Engineering from the Isfahan University of Technology, Isfahan, Iran, in 1993, 1995 and 2000, respectively. In 2001, he joined Shahrekord University, Chaharmahal and Bakhtiari Province, Iran, as an Assistant Professor, and since 2013 he has been an Associate Professor in the Department of Electrical Engineering. His current research interests include smart and micro grids, expert systems, and renewable energy resources and systems.

S. Y. Derakhshandeh received his B.S. degree in Electrical Engineering from the Power and Water University of Technology, Tehran, Iran, in 2003; and his M.S. and Ph.D. degrees in Electrical Engineering from the Isfahan University of Technology, Isfahan, Iran, in 2006 and 2013, respectively. He is presently working as an Assistant Professor in the Department of Engineering, Shahrekord University, Shahrekord, Iran. His current interests include power system analysis, electricity markets and microgrids.